IEEE Photonics Journal
An IEEE Photonics Society Publication

Open Access

Adaptive Thresholding Scheme for Demodulation of Rolling-Shutter Images Obtained in CMOS Image Sensor Based Visible Light Communications

Volume 10, Number 6, December 2018

Chi-Wai Chow
Yen-Chun Liu
Ruei-Jie Shiu
Chien-Hung Yeh

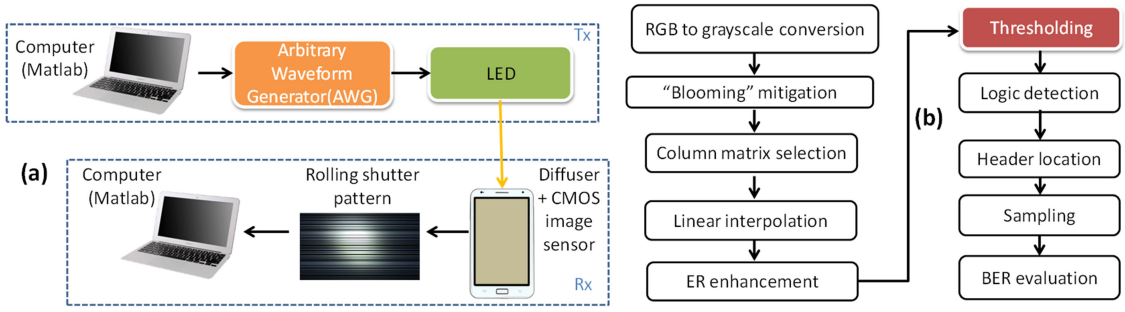

DOI: 10.1109/JPHOT.2018.2876798
1943-0655 © 2018 IEEE

Adaptive Thresholding Scheme for Demodulation of Rolling-Shutter Images Obtained in CMOS Image Sensor Based Visible Light Communications

Chi-Wai Chow,[1] Yen-Chun Liu,[1] Ruei-Jie Shiu,[1] and Chien-Hung Yeh [2]

[1]Department of Photonics and Institute of Electro-Optical Engineering, National Chiao Tung University, Hsinchu 30010, Taiwan
[2]Department of Photonics, Feng Chia University, Taichung 40724, Taiwan

DOI:10.1109/JPHOT.2018.2876798

Manuscript received September 16, 2018; revised October 12, 2018; accepted October 15, 2018. Date of publication October 22, 2018; date of current version November 5, 2018. This work was supported in part by the Ministry of Science and Technology, Taiwan under Grants MOST-107-2221-E-009-118-MY3 and MOST-106-2221-E-009-105-MY3; and in part by Higher Education Sprout Project, and in part by Ministry of Education in Taiwan. Corresponding author: Chi-Wai Chow (e-mail: cwchow@faculty.nctu.edu.tw).

Abstract: Light-emitting-diode transmitter and complementary-metal–oxide–semiconductor (CMOS) image sensor receiver based visible light communication is a promising scheme for an optical wireless communication. During the demodulation of the rolling shutter pattern obtained from the CMOS image sensor Rx, due to the high signal fluctuation introduced by the uneven light exposure, special thresholding schemes are needed to correctly identify the data logic. In this work, we propose and demonstrate a modified adaptive scheme (MQA) for the demodulation of the rolling shutter pattern. Experimental bit-error-ratio (BER) measurements using different thresholding schemes at different illuminance are analyzed. The results show that the proposed MQA scheme can provide much lower BER, with similar process latencies when compared with other schemes.

Index Terms: Light emitting diode (LED), visible light communication (VLC), CMOS image sensor.

1. Introduction

The demand for wireless transmission capacity is increasing rapidly for the past decades. It is becoming more and more difficult to provide high-speed and reliable wireless communication at low cost. As most of the wireless transmissions happen indoors or at fixed locations, there is a high possibility to offload these transmissions to localized access points (AP) using WiFi or visible light communication (VLC). VLC provides many interesting features for wireless communication, allowing it to be applicable for the future 5G and beyond mobile systems [1]. VLC is license-free and electromagnetic-interference (EMI)-free. VLC signal cannot penetrate wall; hence it can increase the wireless transmission security. Recently, different high-speed VLC transmissions based on light emitting diode (LED) transmitter (Tx); and photodiode (PD) receiver (Rx) are demonstrated [2]–[8]. VLC can also offer many interesting applications, such as positioning and navigation [9], underwater transmissions [10]–[12], light-panel and mobile-phone communications [13], [14]. Instead of us-

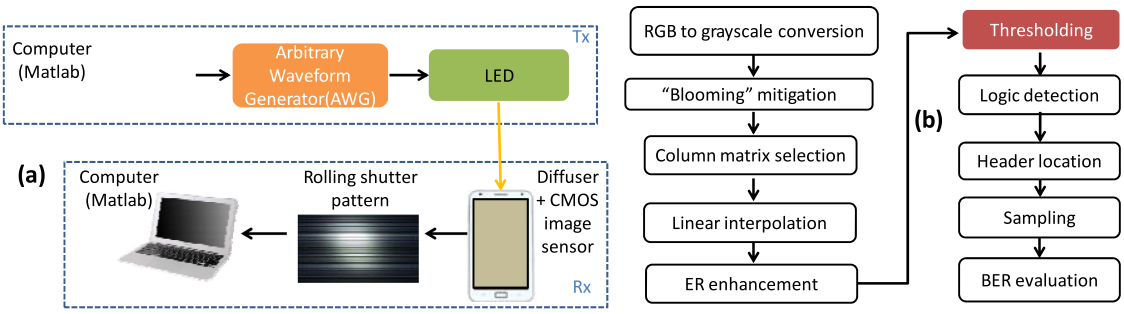

Fig. 1. (a) VLC experimental setup of using white-light LED and mobile-phone based CMOS image sensor; (b) Flow diagram of the processes during the VLC rolling shutter pattern demodulation.

ing PD Rx, using the mobile-phone or car embedded complementary-metal–oxide–semiconductor (CMOS) sensor for Rx is interesting since there is no need to install additional PD to mobile-phone or vehicles. A 3 x 50-bit/s (150-bit/s) red-green-blue (RGB) Tx and CMOS image sensor Rx system has been reported [15]. Besides, a special image sensor with built-in sensing pixels for the images and high-speed VLC was proposed [16]; however, it is not commercially available. By using the rolling shutter operation of the CMOS image sensor [17], the VLC data rate can be significantly increased. Previously, we have demonstrated a VLC packet reconstruction scheme to mitigate the CMOS image sensor frame-to-frame "blind" processing time-gap in order to increase the data rate [18].

During the demodulation of the CMOS image sensor rolling shutter pattern, due to the high signal fluctuation introduced by the uneven light exposure, special thresholding schemes are needed to correctly identify the data logic. Danakis *et al.* [17] and Chow *et al.* [19] illustrated using 2nd and 3rd order polynomial curve fitting respectively for the thresholding of the rolling shutter grayscale pattern. However, these thresholding scheme may not be good enough for demodulating fast changing and high dynamic contrast VLC data. Liu *et al.* [20] reported that quick adaptive (QA) thresholding scheme outperformed the 2nd and 3rd order polynomial curve fitting thresholding. This QA thresholding scheme is based on weighted moving averaging of the rolling shutter grayscale values. However, the QA thresholding by definition only considers the weighted moving average in the prior direction of the rolling shutter pattern. This will produce bit error during demodulation particularly at high illuminance environment. In this work, we propose and demonstrate a modified adaptive scheme (MQA) for the demodulation of the CMOS image sensor rolling shutter pattern. Experimental bit-error-ratio (BER) measurements using different thresholding schemes at different illuminance are analyzed and compared. The results show that the proposed MQA scheme can provide much lower BER, with similar process latencies with other schemes.

2. Algorithms and Experiment

The VLC experimental setup of using white-light LED and mobile-phone based CMOS image sensor is shown in Fig. 1(a). The VLC data in on-off keying (OOK) modulation format is programmed using Matlab, which is stored in an arbitrary waveform generator (AWG, Tektronix AFG3252C). It has an analog bandwidth of 240 MHz and sampling rate of 2 GSample/s. The VLC data is then applied to a white-light phosphor-based LED (Cree XR-E) (color temperature = 5500 K) through the AWG. A mobile-phone (Iphone7) with the 1080 $\times$ 1920 pixels resolution CMOS image sensor is used. The received image frames will be transferred to the Matlab in the computer for demodulation.

During the rolling shutter operation of the mobile-phone CMOS image sensor, the pixel row is activated starting from the top to the bottom. If the LED light is modulated faster than the CMOS image sensor frame rate, bright and dark fringes will be gripped in the image frame representing LED ON and OFF respectively, as illustrated in Fig. 1(a). As the CMOS image sensor has the

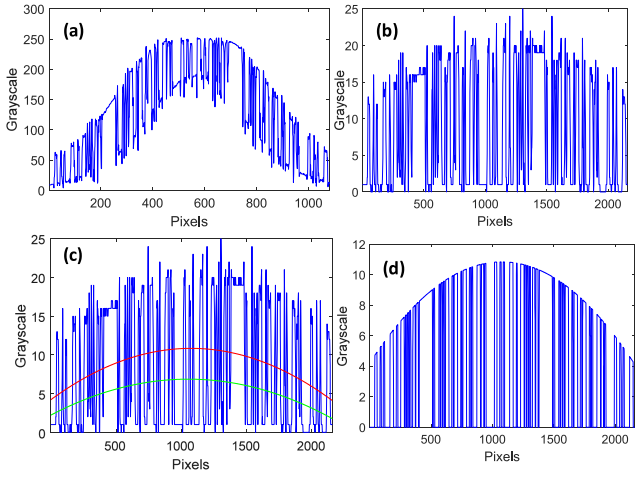

Fig. 2. Grayscale value rolling shutter patterns (a) with "blooming" effect, (b) after "blooming" mitigation, (c) before ER enhancement and (d) after ER enhancement.

resolution of 1080 $\times$ 1920 pixels, there will be 1080 pixel rows. Fig. 1(b) illustrates the processes during the VLC rolling shutter pattern demodulation. The RGB image frames with bright (LED ON) and dark (LED OFF) fringes are transformed into grayscale values format. As there is an uneven light exposure (called "blooming" effect) occurs at the center of the image frame, high grayscale values will be observed even in the dark fringes. Blooming mitigation scheme proposed in ref. [18] is used, and after this, a column matrix of 1080 $\times$ 1 grayscale values can be extracted. This column matrix can be plotted to form the grayscale value rolling shutter pattern. In order to fascinate the rolling shutter pattern demodulation, linear interpolation is used to rise the effective sample points for the rolling shutter pattern. As there is still a high signal fluctuation in the VLC data after the linear interpolation, extinction ration (ER) enhancement scheme is needed. The concept of ER enhancement is to reduce the fluctuation of the grayscale values in the rolling shutter pattern. As illustrated in ref. [21], there are two steps for the ER enhancement. In the first step, a 2nd order polynomial curve fitting is applied to the original grayscale values. When the grayscale values in the original pattern is higher than that in the fitting curve, the original grayscale values will be set to equal to the values of this fitting curve. Then, another 2nd order polynomial fitting curve is generated. The interception points between the grayscale values in the pattern and the second fitting curve are set to zero. After this, the thresholding scheme is applied to distinguish the logic 1 and logic 0. Then, the header location will be located for the VLC packet synchronization, and the BER performance will be evaluated as shown in Fig. 1(b). Fig. 2(a)–(d) show the grayscale value rolling shutter pattern at different demodulation processes. Fig. 2(a) shows the 1080 $\times$ 1 column matrix with "blooming" effect. After "blooming" mitigation, the pattern with more uniform grayscale values can be obtained as shown in Fig. 2(b). Then, ER enhancement using two 2nd order polynomial curve fitting is applied as discussed before as shown in Fig. 2(c). Fig. 2(d) shows the grayscale value pattern after the ER enhancement.

We now discuss the implementation of our proposed MQA thresholding scheme. We also compare this scheme with the QA thresholding scheme [20]. In the previously proposed QA thresholding scheme [20], the thresholding value is obtained by performing the weighted moving average grayscale value in a group, and s is the size of the group in number of pixels. Let y_i be the grayscale value of a pixel at point i. To calculate the weighted moving average, we stress the grayscale values closer to the target value. Then, the threshold in the QA thresholding is represented by Eq. (1), where r is the adjustment ratio.

$$\begin{cases} T_i = r \dfrac{\sum_{n=0}^{s-1} y_{i-n} \left(1 - \frac{1}{s}\right)^n}{\sum_{n=0}^{s-1} \left(1 - \frac{1}{s}\right)^n} \end{cases} \tag{1}$$

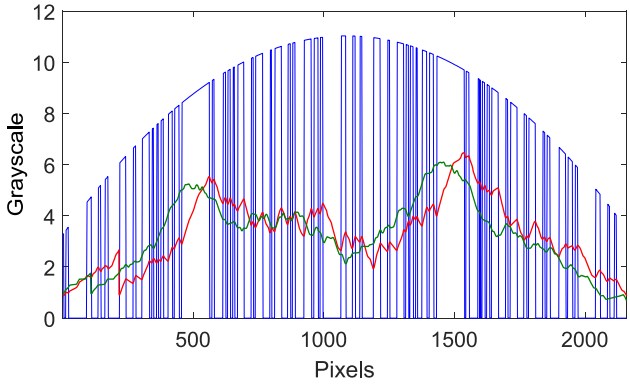

Fig. 3. Grayscale value rolling shutter patterns using QA thresholding (red curve) and MQA (green curve).

We can see that the weighting factor $(1-\frac{1}{s})$ is less than 1 for any natural number of s and this factor will become smaller when n increases. Assume the adjustment ratio r, be 0.8, the threshold value from the QA scheme is shown Eq. (2).

$$\begin{cases} T_i = 0.8\dfrac{\sum_{n=0}^{s-1} y_{i-n}\left(1-\frac{1}{s}\right)^n}{\sum_{n=0}^{s-1}\left(1-\frac{1}{s}\right)^n}, & i \geq s \\ T_i = 0.8\dfrac{\sum_{n=0}^{s-1} y_{i+n}\left(1-\frac{1}{s}\right)^n}{\sum_{n=0}^{s-1}\left(1-\frac{1}{s}\right)^n}, & i < s, \end{cases} \tag{2}$$

However, the QA thresholding by definition [22] only considers the weighted moving average in the prior direction of the rolling shutter pattern. This means the threshold at a particular pixel is predicted from the left-hand-side of the pattern. Here, in our proposed MQA thresholding, we will consider the weighted moving average in both prior and later directions, as shown in Eq. (3). This means the threshold at a particular pixel is predicted from both the left and right-hand-side of the pattern.

$$\begin{cases} T_i = r\dfrac{\sum_{n=-s/2}^{s/2} y_{i+n}\left(1-\frac{1}{s}\right)^{|n|}}{\sum_{n=-s/2}^{s/2}\left(1-\frac{1}{s}\right)^{|n|}} \end{cases} \tag{3}$$

Similarly, when calculating the threshold values during the boundary cases, the MQA thresholding is expressed as Eq. (4), where p is the total number of pixels in the whole grayscale value pattern.

$$\begin{cases} T_i = r\dfrac{\sum_{n=-i+1}^{s/2} y_{i+n}\left(1-\frac{1}{s}\right)^{|n|}}{\sum_{n=-i+1}^{s/2}\left(1-\frac{1}{s}\right)^{|n|}}, & i < \frac{s}{2} \\ T_i = r\dfrac{\sum_{n=-s/2}^{s/2} y_{i+n}\left(1-\frac{1}{s}\right)^{|n|}}{\sum_{n=-s/2}^{s/2}\left(1-\frac{1}{s}\right)^{|n|}}, & \frac{s}{2} \leq i \leq p-\frac{s}{2} \\ T_i = r\dfrac{\sum_{n=-s/2}^{1080-i} y_{i+n}\left(1-\frac{1}{s}\right)^{|n|}}{\sum_{n=-s/2}^{1080-i}\left(1-\frac{1}{s}\right)^{|n|}}, & i > p-\frac{s}{2} \end{cases} \tag{4}$$

3. Results and Discussions

Fig. 3 shows grayscale value rolling shutter patterns using QA (red curve) and MQA (green curve). We can observe that when QA thresholding is used (red curve), a strictly increasing thresholding will be obtained at the pixels around 500th and 1500th, which have higher illuminance. This is because the QA thresholding only considers the weighted moving average in the prior direction of the rolling shutter pattern. When the MQA thresholding is used (green curve), we can observe that

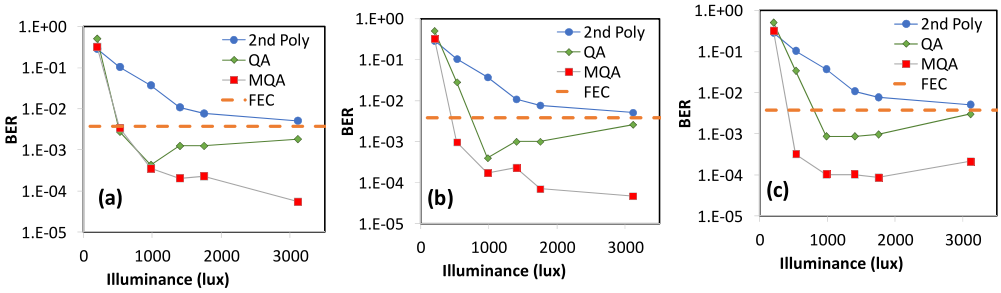

Fig. 4. BER performances using different thresholding schemes under different illuminance when the group size s: (a) 360 pixels, (b) 432 pixels, (c) 540 pixels.

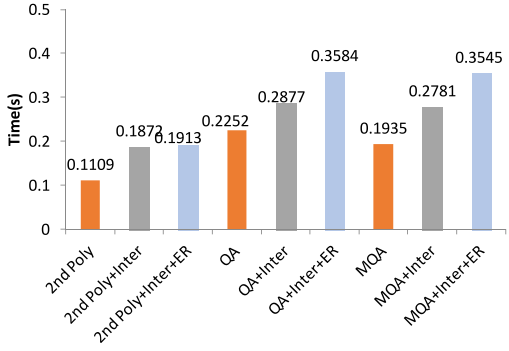

Fig. 5. Measured processing latencies of the 2nd order polynomial curve fitting, QA and MQA thresholding schemes.

the strictly increasing thresholding can be avoided at pixels around 500th and 1500th since it will consider the weighted moving averaging in both directions.

BER evaluations are performed by using the 2nd polynomial curve fitting, QA and MQA thresholding schemes. For the three thresholding schemes, the processes of "blooming" mitigation, linear interpolation, ER enhancement are used. Fig. 4(a)–(c) show the BER performances using different thresholding schemes under different illuminance when the group size $s = 360$ pixels, 432 pixels and 540 pixels. They corresponds to dividing the grayscale value rolling shutter pattern into 6, 5, and 4 groups respectively. The lux is varied by adjusting the transmission distance between the LED and the mobile-phone. Although the QA can satisfy the forward error correction (FEC) requirement of BER $= 3.8 \times 10^{-3}$, MQA can have around one order of magnitude BER improvement, particularly at high illuminance scenarios. In this experiment, 128-bit VLC packet is used, and the frame rate of the CMOS camera is 60 fps. Hence the data rate of the system is 7.68 kbit/s.

Experiments using one round LED and 2 round LEDs put side-by-side to emulate a long-shaped LED are performed, and the results show that as long as the LED light source is located at the center of the CMOS image sensor, the ER enhancement algorithm and the MQA can work properly when using a round LED or a long-shaped LED. Results also show that when only part of the LED light source is received by the CMOS image sensor, the proposed ER enhancement scheme may not working properly.

We also compare the processing latencies of the three thresholding schemes under test as shown in Fig. 5. In each scheme, the time needed for the thresholding alone, the thresholding together with the linear interpolation, and the thresholding plus the linear interpolation and the ER enhancement are included for comparison. The computer used to run these processes has an Intel i7 processor with 64 GB random access memory (RAM). We can observe that the 2nd order polynomial curve fitting takes the less time, but the BER performance is the poorest among them. We can also observe that the proposed MQA scheme takes similar processing time when compared with the QA scheme; however the MQA scheme can outperform others in BER evaluation. In this proof-

of-concept experiment, the transmission distance is limited to around 30 cm. Longer transmission distance could be achieved by using a LED array to increase the illumination area and intensity. There are several potential applications of the proposed VLC system, such as distributing menus in foot courts/restaurants, sending leaflets in department stores/museums, and providing indoor navigation information via VLC.

4. Conclusion

We proposed and demonstrated a MQA thresholding scheme for the demodulation of the CMOS image sensor rolling shutter pattern in VLC systems. Experimental results showed that the proposed MQA thresholding scheme can satisfy the FEC requirement, and can have around one order of magnitude BER improvement when compared with the typical QA thresholding scheme. We have discussed the implementation and analyzed the proposed MQA thresholding scheme. Measurement results also showed that the proposed MQA scheme needed similar processing time when compared with the QA scheme.

References

[1] S. Wu, H. Wang, and C. H. Youn, "Visible light communications for 5G wireless networking systems: From fixed to mobile communications," *IEEE Netw.*, vol. 28, no. 6, pp. 41–45, Nov./Dec. 2014.
[2] N. Chi, Y. Zhou, J. Shi, Y. Wang, and X. Huang, "Enabling technologies for high speed visible light communication," in *Proc. Int. Conf. Opt. Fiber Commun.*, 2017, Paper Th1E. 3.
[3] H. L. Minh *et al.*, "100-Mb/s NRZ visible light communications using a post-equalized white LED," *IEEE Photon. Technol. Lett.*, vol. 21, no. 15, pp. 1063–1065, Aug. 2009.
[4] J. Vučić, C. Kottke, S. Nerreter, K. D. Langer, and J. W. Walewski, "513 Mbit/s visible light communications link based on DMT-modulation of a white LED," *J. Lightw. Technol.*, vol. 28, no. 24, pp. 3512–3518, Dec. 2010.
[5] Z. Wang, C. Yu, W. D. Zhong, J. Chen, and W. Chen, "Performance of a novel LED lamp arrangement to reduce SNR fluctuation for multi-user visible light communication systems," *Opt. Exp.*, vol. 20, pp. 4564–4573, 2012.
[6] W. Y. Lin *et al.*, "10 m/500 Mbps WDM visible light communication systems," *Opt. Exp.*, vol. 20, pp. 9919–9924, 2012.
[7] C. Hsu, C. Chow, I. Lu, Y. Liu, C. Yeh, and Y. Liu, "High speed imaging 3 × 3 MIMO phosphor white-light LED based visible light communication system," *IEEE Photon. J.*, vol. 8, no. 6, Dec. 2016, Art. no. 7907406.
[8] C. W. Chow, C. H. Yeh, Y. F. Liu, and P. Y. Huang, "Background optical noises circumvention in LED optical wireless systems using OFDM," *IEEE Photon. J.*, vol. 5, no. 2, Apr. 2013, Art. no. 7900709.
[9] C. W. Hsu *et al.*, "Visible light positioning and lighting based on identity positioning and RF carrier allocation technique using a solar cell receiver," *IEEE Photon. J.*, vol. 8, no. 4, Aug. 2016, Art. no. 7905507.
[10] H. H. Lu *et al.*, "An 8 m/9.6 Gbps underwater wireless optical communication system," *IEEE Photon. J*, vol. 8, no. 5, Oct. 2016, Art. no. 7906107.
[11] T. C. Wu, Y. C. Chi, H. Y. Wang, C. T. Tsai, and G. R. Lin, "Blue laser diode enables underwater communication at 12.4 Gbps," *Sci. Rep.*, vol. 7, 2017, Art. no. 40480.
[12] C. Wang, H. Y. Yu, and Y. J. Zhu, "A long distance underwater visible light communication system with single photon avalanche diode," *IEEE Photon. J.*, vol. 8, no. 5, Oct. 2016, Art. no. 7906311.
[13] C. W. Chow *et al.*, "Secure mobile-phone based visible light communications with different noise-ratio light-panel," *IEEE Photon. J.*, vol. 10, no. 2, Apr. 2018, Art. no. 7902806.
[14] C. W. Chow *et al.*, "Using advertisement light-panel and CMOS image sensor with frequency-shift-keying for visible light communication," *Opt. Exp.*, vol. 26, pp. 12530–12535, 2018.
[15] P. Luo *et al.*, "Experimental demonstration of RGB LED-based optical camera communications," *IEEE Photon. J.*, vol. 7, no. 5, Oct. 2015, Art. no. 7904242.
[16] I. Takai, S. Ito, K. Yasutomi, K. Kagawa, M. Andoh, and S. Kawahito, "LED and CMOS image sensor based optical wireless communication system for automotive applications," *IEEE Photon. J.*, vol. 5, no. 5, Oct. 2013, Art. no. 6801418.
[17] C. Danakis, M. Afgani, G. Povey, I. Underwood, and H. Haas, "Using a CMOS camera sensor for visible light communication," in *Proc. Int. Conf. IEEE Globecom*, 2012, pp. 1244–1248.
[18] W. C. Wang, C. W. Chow, C. W. Chen, H. C. Hsieh, and Y. T. Chen, "Beacon jointed packet reconstruction scheme for mobile-phone based visible light communications using rolling shutter," *IEEE Photon. J.*, vol. 9, no. 6, Dec. 2017, Art. no. 7907606.
[19] C. W. Chow, C. Y. Chen, and S. H. Chen, "Enhancement of signal performance in LED visible light communications using mobile phone camera," *IEEE Photon. J.*, vol. 7, no. 5, Oct. 2015, Art. no. 7903607.
[20] Y. Liu *et al.*, "Comparison of thresholding schemes for visible light communication using mobile-phone image sensor," *Opt. Express.*, vol. 24, pp. 1973–1978, 2016.
[21] Y. Liu, H. Y. Chen, K. Liang, C. W. Hsu, C. W. Chow, and C. H. Yeh, "Visible light communication using receivers of camera image sensor and solar cell," *IEEE Photon. J.*, vol. 8, no. 1, Feb. 2016, Art. no. 7800107.
[22] P. D. Wellner, "Adaptive thresholding for the digital desk," Rank Xerox Res. Centre, Cambridge Lab., Cambridge, U. K., Tech. Rep. EPC-93-110, 1993.